Synthesis and Characterization of PEGylated Toll Like Receptor 7 Ligands

Michael Chan, **Tomoko Hayashi**[*], **Richard D. Mathewson**, **Shiyin Yao**, **Christine Gray**, **Rommel Tawatao**, **Kevin Kalenian**, **Yanmei Zhang**, **Yuki Hayashi**, **Fitzgerald S. Lao**, **Howard B. Cottam**, and **Dennis A. Carson**

Moores Cancer Center, University of California San Diego, 3855 Health Science Drive, La Jolla California 92093-0820

Abstract

Toll like receptor 7 (TLR7) is located in the endosomal compartment of immune cells. Signaling through TLR7, mediated by the adaptor protein MyD88, stimulates the innate immune system and shapes adaptive immune responses. Previously, we characterized TLR7 ligands conjugated to protein, lipid or polyethylene glycol (PEG). Among the TLR7 ligand conjugates, the addition of PEG chains reduced the agonistic potency. PEGs are safe in humans and widely used for improvement of pharmacokinetics in existing biologics and some low molecular weight compounds. PEGylation could be a feasible method to alter the pharmacokinetics and pharmacodynamics of TLR7 ligands. In this study, we systematically studied the influence of PEG chain length on the *in vitro* and *in vivo* properties of potent TLR7 ligands. PEGylation increased solubility of the TLR7 ligands and modulated protein binding. Adding a 6–10 length PEG to the TLR7 ligand reduced its potency toward induction of interleukin (IL)-6 by murine macrophages *in vitro* and IL-6 and tumor necrosis factor (TNF) *in vivo*. However, PEGylation with 18 or longer chain restored, and even enhanced, the agonistic activity of the drug. In human peripheral blood mononuclear cells, similar effects of PEGylation were observed for secretion of proinflammatory cytokines, IL-6, IL-12, TNF-α, IL-1β and type 1 interferon, as well for B cell proliferation. In summary, these studies demonstrate that conjugation of PEG chains to a synthetic TLR ligand can impact its potency for cytokine induction depending on the size of the PEG moiety. Thus, PEGylation may be a feasible approach to regulate the pharmacological properties of TLR7 ligands.

Keywords

polyethylene glycol; PEG; Toll like receptor 7

Introduction

The 13 known mammalian Toll-like receptors (TLRs) are key sensors for pathogen-associated molecular patterns (PAMPs) that are expressed by both exogenous microbes and self components. Activation of TLRs induces innate and adaptive immune responses (1). The various TLRs interact with lipoprotein (TLR2), double stranded RNA (TLR3), lipopolysaccharide (LPS, TLR4), flagellin (TLR5), single stranded RNA (TLR7/8), and

---

unmethylated CpG DNA (TLR9). All TLRs, except TLR3, signal through the adaptor protein MyD88, which leads to activation of nuclear factor kappa β (NFκB) and mitogen activated protein kinases (MAPK) to induce production of pro-inflammatory cytokines such as IL-1β, IL-6, IL-12 and tumor necrosis factor (TNF)-α (2,3). The natural ligand for TLR7 was identified as guanine and uridine-rich single stranded RNA (4). In addition, several low molecular weight activators of TLR7 have been discovered, including imidazoquinolines, and purine-like molecules (5–7). Among the latter, 9-benzyl-8-hydroxy-2-(2-methoxyethoxy) adenine (SM360320; designated here as **1V136**), has been shown to be a potent and specific TLR7 agonist (8).

An important aspect of TLR biology is the connection between receptor localization, cell activation, and cytokine production (9). TLR7 and TLR9 are only active when proteolytically processed and loaded into endosomes. The active form of TLR7 is located mainly in the endosomal compartment of innate immune cells, including dendritic cells, macrophages, mast cells, and B lymphocytes (2,7), which may regulate organelle trafficking differently. The conjugation of various chemical entities to phospholipids is known to facilitate endocytosis. In a previous study, we conjugated a TLR7 ligand to various moieties, including phospholipid, polyethylene glycol (PEG), and albumin, and studied how the conjugates influenced drug potency (10,11). Conjugation of TLR7 ligand to phospholipids or albumin increased its potency 10 to 100 fold *in vitro* and improved its pharmacodynamics *in vivo*. Furthermore, the phospholipid conjugate was a powerful adjuvant for vaccination that induced antibody responses within 14 days after primary immunization, and that stimulated both antibody production and antigen specific interferon production. In contrast, the conjugation of the same TLR7 ligand to PEG reduced its cytokine inducing potency *in vitro* (11).

PEG is approved by the Food and Drug Administration for internal use. PEG is not immunogenic itself and is highly soluble in water. The initial motivation to further study the PEGylated TLR7 ligand was due to poor water solubility of the heterocyclic molecule. We reasoned that PEGylation might improve the water solubility and in turn improve the bioavailability of the ligand. Although adding PEG chain to TLR7 ligand improved solubility, the addition of short (6–10) PEG chains significantly reduced the agonistic potency of the compounds (11). Here, we hypothesized that the agonist activity might be influenced by length of the PEG chain attached to TLR7 ligand, because of the unique endosomal localization of TLR7. We conjugated TLR7 ligands to PEG chains of various lengths from 6 to over 470 PEG units and characterized their *in vitro* and *in vivo* pharmacokinetics and pharmacodynamics.

Experimental Procedures

Reagents

Sunbright® MEPA-20H, Sunbright® MEPA-50H, Sunbright® MEPA-12T, Sunbright® MEPA-20T PEGs were purchased from NOF America Corporation (White Plains, NY). *O*-(2-Aminoethyl)-*O′*-(2-azidoethyl)pentaethylene glycol, *O,O′*-Bis(2-aminoethyl)octadecaethylene glycol and *O*-(2-Aminoethyl)-*O′*-(2-azidoethyl)nonaethylene glycol and all other reagents were purchased as at least reagent grade from Sigma-Aldrich (St. Louis, MO) without further purification. Solvents were purchased from Fischer Scientific (Pittsburgh, PA) and were either used as purchased or redistilled with an appropriate drying agent.

1,2-Dioleoyl-sn-glycero-3-phosphoethanolamine (DOPE) was purchased from Avanti Polar Lipids (Alabaster, AL). All other reagents were purchased as at least reagent grade from

Sigma-Aldrich (St. Louis, MO) without further purification. Ovalbumin (OVA, grade V) was purchased from Sigma-Aldrich.

Endotoxin levels in the reagents and conjugates used for experiments of immunological activities were measured using the QCL1000® Endpoint Chromogenic Limulus Amoebocyte Lysate (LAL) assay purchased from BioWhittaker (Walkerville, MD). Reagents that contained less than 1 pg endotoxin per μg protein or compound were used throughout the experiments.

All conjugates were lyophilized to a dry powder if possible and stored at −20 °C. All others were stored as viscous oils at −20 °C. The conjugates were dissolved in DMSO at 50 to 100mM and further diluted before immunological assays.

Chemistry

Instrumentation—Analytical TLC was performed using precoated TLC silica gel 60 F254 aluminum sheets purchased from EMD (Gibbstown, NJ) and visualized using UV light. Flash chromatography was carried out on EMD silica gel 60 (40–63 μm) system or with a Biotage Isolera One (Charlotte, NC) using the specified solvent. Chromatography and mass spectra (ESI) were recorded on an 1100 LC/MSD (Agilent Technologies, Inc., Santa Clara, CA) with a Supelco Discovery HS C18 column (Sigma-Aldrich). ^{1}H NMR spectra were obtained on a Varian Mercury Plus 400 or on a Varian Inova 500 (Varian, Inc., Palo Alto, CA). The chemical shifts are expressed in parts per million (ppm) using suitable deuterated NMR solvents in reference to TMS at 0 ppm. Osmolalities were measured on the Advanced Micro-Osmometer Model 3M0 Plus (Advanced Instruments, Inc, Norwood, MA) and are expressed in mosmoles of solute per kg of solvent (12). Absorbance values for protein binding assays were measured with a TECAN Infinite M200 (TECAN Instruments, Durham, NC).

4-((6-amino-8-hydroxy-2-(2-methoxyethoxy)-9H-purin-9-yl)methyl)-N-(20-azido-3,6,9,12,15,18-hexaoxaicosyl)benzamide(1a)—To a solution of 4-{[6-Amino-2-(2-methoxyethoxy)-8-oxo-7H-purin-9(8H)-yl]methyl}benzoic Acid (**1V209**) (0.233 g, 0.648 mmol) in anhydrous DMF (3 mL) was added HATU (0.271 g, 0.713 mmol) and anhydrous TEA (181 μL, 1.3 mmol). A solution of O-(2-Aminoethyl)-O'-(2-azidoethyl)pentaethylene glycol, O,O'-Bis(2-aminoethyl)octadecaethylene glycol (0.25 g, 0.713 mmol) in anhydrous DMF (1 mL) was prepared and slowly added to the reaction mixture. The reaction mixture was stirred at room temperature until completion and then evaporated in vacuo. The product was purified by flash chromatography using 8% MeOH in DCM to give 0.465 g of an opaque oil in 91% yield. Rt) 11.9 min. ^{1}H NMR (500 MHz, DMSO-$d6$) δ (ppm): 10.00 (s, 1H), 8.48 (t, J = 5.49 Hz, 1H), 7.78 (d, J = 8.24 Hz, 2H), 7.34 (d, J = 8.24, 2H), 6.50 (s, 2H), 4.90 (s, 2H), 4.24 (t, J = 4.55, 2H), 3.57 (broad m, 4H), 3.486 (broad m, 22H), 3.39 (m, 4H), 3.26 (s, 3H). ESI-MS (positive ion mode): calculated for $C_{30}H_{45}N_9O_{10}$ m/z [M+1] 692.73; found 692.58.

3-(1-(1-(4-((6-amino-8-hydroxy-2-(2-methoxyethoxy)-9H-purin-9-yl)methyl)phenyl)-1-oxo-5,8,11,14,17,20-hexaoxa-2-azadocosan-22-yl)-1H-1,2,3-triazol-4-yl)propanoic acid (1b)—Compound **1a** (50 mg, 72 μmol) and 4-pentynoic acid (21 mg, 210 μmol) was dissolved in 1:1 t-butanol/H2O (1 mL) and THF (0.5 mL). Sodium ascorbate (5.8 mg, 29.2 μmol) and Cu(OAc)$_2$ (2.6 mg, 14.3 μmol) in 1:1 t-butanol/H2O (1 mL) was slowly added to the reaction mixture and stirred at room temperature until compound **1a** was fully reacted by TLC. The product was extracted with DCM (10 mL) and H2O (10 mL), and the organic layer was dried over MgSO$_4$. The product was further purified by flash chromatography with 10:1:89 MeOH:acetic acid:DCM and

lyophilized to give 167 mg of a slightly yellow solid in 95% yield. Rt) 11.35 min. ^{1}H NMR (500 MHz, DMSO-*d6*) δ (ppm): 8.44 (t, *J* = 5.34 Hz, 1H), 7.77 (d, *J* = 7.93 Hz, 2H), 7.77 (s, 1H), 7.34 (d, *J* = 7.93 Hz, 2H), 4.88 (s, 2H), 4.40 (t, *J* = 5.03 Hz, 2H), 4.23 (t, *J* = 4.60Hz, 2H), 3.72 (t, *J* = 5.03 Hz, 2H), 3.57 (t, *J* = 4.60 Hz, 2H), 3.51 (broad m, 6H), 3.44 (broad m, 4H), 3.38 (broad m, 14H), 3.26 (s, 3H), 2.80 (t, *J* = 7.02 Hz, 2H), 2.30 (t, *J* = 7.05 Hz, 2H). ESI-MS (positive ion mode): calculated for $C_{35}H_{51}N_9O_{12}$ m/z [M+1] 790.83; found 790.59.

4-((6-amino-8-hydroxy-2-(2-methoxyethoxy)-9H-purin-9-yl)methyl)-N-(20-amino-3,6,9,12,15,18-hexaoxaicosyl)benzamide(1c)—To a solution of compound **1a** (50 mg, 72μmol) in MeOH (1 mL) was added Raney Ni and stirred at room temperature under H_2 atmosphere for 2 hr. Raney Ni was filtered and the product was purified by flash chromatography with 10% MeOH in DCM to give a white solid in quantitative yield. RT = 10.55 min. ^{1}H NMR (500 MHz, DMSO-*d6*) δ (ppm): 8.48 (t, *J* = 5.19 Hz, 1H), 7.78 (d, *J* = 7.32 Hz, 2H), 7.35 (d, *J* = 7.63 Hz, 2H), 6.53 (s, 2H), 4.90 (s, 2H), 4.24 (t, *J* = 4.25 Hz, 2H), 3.57 (t, *J* = 5.2 Hz, 2H), 3.54 (broad m, 24H), 3.40 (t, *J* = 5.2 Hz, 2H), 3.26 (s, 3H), 2.97 (t, *J* = 4.73 Hz, 2H). ESI-MS (positive ion mode): calculated for $C_{30}H_{47}N_7O_{10}$*m/z* [M+1] 666.74; found 666.61.

4-((6-amino-8-hydroxy-2-(2-methoxyethoxy)-9H-purin-9-yl)methyl)-N-(32-azido-3,6,9,12,15,18,21,24,27,30-decaoxadotriacontyl)benzamide (2a)—To a solution of 4-{[6-Amino-2-(2-methoxyethoxy)-8-oxo-7*H*-purin-9(8*H*)-yl]methyl}benzoic Acid (0.100 g, 0.278 mmol) in anhydrous DMF (5 mL) was added HATU (0.117 g, 0.306 mmol) and anhydrous TEA (77.014 mL, 0.556 mmol). A solution of *O*-(2-aminoethyl)-*O*′-(2-azidoethyl)nonaethylene glycol (0.150 g, 0.306 mmol) in anhydrous DMF (1 mL) was prepared and slowly added to the reaction mixture. The reaction mixture was stirred at room temperature until completion and then evaporated in vacuo. The product was purified by flash chromatography using 5% MeOH in DCM to give 0.224 g of an opaque oil in 93% yield. Rt = 12 min. ^{1}H NMR (400 MHz, DMSO-d$_6$) δ (ppm): 10.01 (s, 1H), 8.45 (t, *J* = 5.6 Hz, 1H), 7.78 (d, *J* = 8.3 Hz, 2H), 7.35 (d, *J* = 8.3 Hz, 2H), 6.49 (s, 2H), 4.90 (s, 2H), 4.25 (t, *J* = 4 Hz, 2H), 3.57 (m, 4H), 3.5 (m, 36H), 3.4 (M, 6H), 3.26 (s, 3H). ESI-MS (positive ion mode): calculated for $C_{38}H_{61}N_9O_{14}$*m/z* [M+1]868.94; found 868.59.

3-(1-(1-(4-((6-amino-8-hydroxy-2-(2-methoxyethoxy)-9H-purin-9-yl)methyl)phenyl)-1-oxo-5,8,11,14,17,20,23,26,29,32-decaoxa-2-azatetratriacontan-34-yl)-1H-1,2,3-triazol-4- yl)propanoic acid(2b)—Compound **2a** (0.218 g, 0.251 mmol) and 4-pentynoic acid (0.074 g, 0.753 mmol) was dissolved in 1:1 t-butanol:H$_2$O (3 mL). Sodium ascorbate (0.02 g, 100 mmol) and Cu(OAc)$_2$ (0.009 g,50 mmol) in 1:1 t-butanol:H$_2$O (1 mL) was slowly added to the reaction mixture and stirred at room temperature until compound **2a** was fully reacted by TLC. The product was extracted with DCM (10 mL) and H$_2$O (10 mL) and the organic layer was dried over MgSO$_4$ to give 0.230 g of an opaque oil in 95% yield. Rt = 11.5 min. ^{1}H NMR (400 MHz, DMSO-d$_6$) δ (ppm): 13.48 (s, 1H), 7.76 (d, *J* = 8.29 Hz, 2H), 7.75 (s, 1H), 7.23 (d, *J* = 8.29, 2H), 4.88 (s, 2H), 4.41 (t, *J* = 5.12 Hz, 2H), 4.23 (t, *J* = 4 Hz, 2H), 3.74 (t, *J* = 5.12 Hz, 2H), 3.57 (t, *J* = 4 Hz, 2H), 3.51 (m, 8H), 3.42 (m, 36H), 3.26 (s, 3H), 2.79 (t, *J* = 7.56 Hz, 2H), 2.24 (t, *J* = 7.56 Hz, 2H). ESI-MS (positive ion mode): calculated for $C_{43}H_{67}N_9O_{16}$*m/z* [M+1]966.04; found 966.67.

4-((6-amino-8-hydroxy-2-(2-methoxyethoxy)-9H-purin-9-yl)methyl)-N-(32-amino-3,6,9,12,15,18,21,24,27,30-decaoxadotriacontyl)benzamide(2c)—To a solution of compound **1a** (50 mg, 57.6μmol) in MeOH (1 mL) was added Raney Ni and stirred at room temperature under H_2 gas for 2 hr. Raney Ni was filtered and the product was purified by flash chromatography with 10% MeOH in DCM to give 30 mg of a white solid

in 62% yield. Rt = 11.1. ^{1}H NMR (400 MHz, DMSO-d$_6$) δ (ppm): 8.48 (t, J = 5.49 Hz, 1H), 7.79 (d, J = 8.24 Hz, 2H), 7.34 (d, J = 8.24 Hz, 2H), 6.53 (s, 2H), 4.9 (s, 2H), 4.24 (t, J = 4.90 Hz, 2H), 3.57 (t, J = 4.90 Hz, 2H), 3.50 (broad m, 40H), 3.38 (m, 4H), 3.26 (s, 3H). ESI-MS (positive ion mode): calculated for $C_{38}H_{63}N_7O_{14}$ m/z [M+1] 842.95; found 842.61.

4-((6-amino-8-hydroxy-2-(2-methoxyethoxy)-9H-purin-9-yl)methyl)-N-(59-amino-3,6,9,12,15,18,21,24,27,30,33,36,39,42,45,48,51,54,57-nonadecaoxanonapentacontyl)benzamide(3)

—Dissolve *O*-(2-Aminoethyl)-*O′*-(2-azidoethyl)nonaethylene glycol (250 mg, 279 μmol) in DMF (30 mL) and stir vigorously at room temperature. In a separate flask combine HATU (38.9 mg, 102 μmol), 4-{6-Amino-2-(2-methoxyethoxy)-8-oxo-7*H*-purin-9(8*H*)-yl]methyl}benzoic Acid (33.4 mg, 93 μmol) and TEA (26 μL, 186 μmol) in DMF (20 mL) and stir for 15 min. Add solution of benzoic acid to the reaction mixture dropwise over 1 hour and stir vigorously at room temperature until benzoic acid is completely reacted. Concentrate and purify product by flash chromatography with 10% MeOH in DCM to give 33 mg in 29% yield. Rt) 11.7 min. ^{1}H NMR (400 MHz, DMSO-d$_6$) δ (ppm): 8.48 (t, J = 5.49 Hz, 1H), 7.79 (d, J = 8.24 Hz, 2H), 7.35 (d, J =7.93 Hz, 2H), 6.52 (s, 2H), 4.90 (s, 2H), 4.24 (t, J = 4.60 Hz, 2H), 3.58 (broad m, 8h), 3.50 (broad m, 70H), 3.39 (m, 4H), 3.26 (s, 3H), 2.97 (t, J = 5.19 Hz, 2H). ESI-MS (positive ion mode): calculated for $C_{56}H_{99}N_7O_{23}$ m/z [M+1] 1239.42; found 1239.72.

Compound 4—To a solution of 4-{[6-Amino-2-(2-methoxyethoxy)-8-oxo-7*H*-purin-9(8*H*)-yl]methyl}benzoic acid (41 mg, 114 μmol), HATU (48 mg, 125 μmol), TEA (35 μL, 228μmol) were combined in DMF (5 mL) was added Sunbright MEPA-20H (250 mg, 125μmol) in DCM (1 mL). The reaction mixture was stirred at room temperature until completion and evaporated to dryness. The product was purified by product by flash chromatography with 10% MeOH in DCM to give 259 mg of a viscous colorless oil in 90% yield. Rt) 13.0 min.

Compound 5—To a solution of 4-{[6-Amino-2-(2-methoxyethoxy)-8-oxo-7*H*-purin-9(8*H*)-yl]methyl}benzoic acid (33 mg, 91 μmol), HATU (38.4 mg, 101 μmol), TEA (26 μL, 182μmol) were combined in DMF (5 mL) was added Sunbright MEPA-50H (500 mg, 101μmol) in DCM (1 mL). The reaction mixture was stirred at room temperature until completion and evaporated to dryness. The product was purified by product by flash chromatography with a stepwise gradient starting from 5% MeOH in DCM to 15% MeOH in DCM to give 419 mg of a viscous colorless oil in 82% yield. Rt) 13.6 min.

Compound 6—To a solution of 4-{[6-Amino-2-(2-methoxyethoxy)-8-oxo-7*H*-purin-9(8*H*)-yl]methyl}benzoic acid (13.6 mg, 38 μmol), HATU (15.8 mg, 42 μmol), TEA (10.6 μL, 76μmol) were combined in DMF (5 mL) was added Sunbright MEPA-12T (500 mg, 42μmol) in DCM (1 mL). The reaction mixture was stirred at room temperature until completion and evaporated to dryness. The product was purified by product by flash chromatography with a stepwise gradient starting from 5% MeOH in DCM to 20% MeOH in DCM to give 380 mg of a viscous colorless oil in 80% yield. Rt) 13.7 min.

Compound 7—To a solution of 4-{[6-Amino-2-(2-methoxyethoxy)-8-oxo-7*H*-purin-9(8*H*)-yl]methyl}benzoic acid (16.3 mg, 45 μmol), HATU (19 mg, 50 μmol), TEA (12.5 μL, 90μmol) were combined in DMF (5 mL) was added Sunbright MEPA-20T (1 g, 50μmol) in DCM (1 mL). The reaction mixture was stirred at room temperature until completion and evaporated to dryness. The product was purified by product by flash chromatography with a stepwise gradient starting from 10% MeOH in DCM to 30% MeOH in DCM to give 786 mg of a viscous colorless oil in 80% yield. Rt) 13.7 min.

Solubility study

Saturated solutions of compounds **1V136, 1V209, 1b**, and **4** were prepared by dissolving excess solids in 100 μL of deionized water. The solutions were mixed and sonicated, and more solid was added if dissolution was incomplete. Samples were centrifuged and separated from the precipitate. Aliquots were taken from these samples and analyzed in an osmometer to determine the milliosmoles (mOsm) of solute per kg of solvent. Silver oxide, and 10% saturated sodium chloride were used for calibration.

Protein binding assay

The protein binding profiles of unconjugated or PEGylated TLR7 ligands (**1V136, 1V209, 1a, 1b, 1c, 2a, 2b, 2c,, 3** and **4**) to dialyzed serum proteins were determined using a rapid equilibrium dialysis device (Pierce Biotechnology, Rockford, IL). Naproxen was purchased from Sigma-Aldrich (St. Louis, MO) and used as a positive control without further purification. Wells without compounds were used as a negative control. Dialyzed fetal bovine serum (FBS) was purchased from Atlanta Biological (Lawrenceville, GA). The samples were prepared and tested according to the manufacture's protocol. Briefly, after equilibrium, samples were precipitated with 95% cold MeOH in water to remove protein and the supernatant UV absorption was measured with a TECAN infinite F2000 at 282 nm with 650 nm as reference.

Animals

6–8 week old femaleC57BL/6 mice were purchased from Charles River Laboratories (San Diego, CA). TLR7 deficient mice (C57BL/6 background) were a gift from Dr. S. Akira, (Osaka University, Osaka, Japan) and were backcrossed ten generations onto the C57BL/6 background. Animals were bred and maintained at UCSD in rooms at $22 \pm 0.5°C$ on a 12:12-hour light-dark cycle from 7 am to 7 pm. All procedures and protocols were approved by the Institutional Animal Care and Use Committee.

In vitro measurements of NFkB activation using NFκB-bla Raw 264.7 Cells

NFκB-bla Raw 264.7 cells were purchased from Life Technologies Corporation (Carlsbad, CA). Cells were harvested, resuspended in Assay Medium (99.5% OptiMEM; 0.5% dialyzed FBS; 0.1 mM non-essential amino acids; 1 mM sodium pyruvate; 10 mM HEPES pH 7.3; 100 U/mL penicillin; 100 μg/mL streptomycin) and then plated in 96-well plates at 5×10^4 per well. Drugs were dissolved and diluted in DMSO to obtain an initial stock solution (10 or 50 mM). Compounds were then serially diluted in DMSO and further diluted in assay medium and added to cells already in each well. Cells were then incubated for approximately 16 hours in 5% CO_2 at 37° C. The NFκB activation was measured according to the manufacturer's protocol using a TECAN Infinite M200 plate reader at an excitation wavelength of 405 nm, and emission wavelengths of 465 nm and 535 nm.

In vitro cytokine induction in bone marrow derived macrophages (BMDM)

BMDM were prepared from C57BL/6 mice as described (10). BMDM were plated in 96-well plates at 200 μl (5×10^4 cells) per well and incubated with the conjugates for 18 hours at 37°C, 5% CO_2, after which time culture supernatants were collected. The levels of cytokines (IL-6, IL-12 or TNF-α) in the supernatants were determined by ELISA (BD Biosciences, La Jolla, CA) (10). Minimum detection levels of these cytokines were 15 pg/mL.

In vitro activities in human peripheral blood mononuclear cells (PBMC)

Human PBMC were isolated from buffy coats obtained from the San Diego Blood Bank (San Diego, CA) as described previously (13). PBMC (1×10^6/mL) were incubated with various compounds for 18 hours at 37°C, 5 % CO_2 and culture supernatants were collected.

The levels of cytokines (IL-6, TNF-α, or IFNα1) in the supernatants were determined by Luminex bead assays (Invitrogen, Carlsbad, CA). The minimum detection levels of IL-6, TNF-α and IFNα1 were 6 pg/mL, 10 pg/mL and 15 pg/mL, respectively.

To evaluate the capability of the conjugates to induce B cell proliferation, PBMC were labeled with 10μM carboxy-fluoresceindiacetatesuccinimidyl ester (CFSE) in saline for 10 min (14). The washed cells were incubated with 1 or 10 μM unconjugated or PEGylated TLR7 ligands for four days. The cells were then surface stained for CD19 to identify B cells. Flow cytometry analysis was performed using FACS Calibur cytometer (BD Biosiences), and the data were analyzed using FlowJo software (Ashland, OR).

Pharmacokinetic (PK) Study

Mice were intravenously (i.v.) injected with 500 nmol unconjugated or PEGylated TLR7 ligands. The serum samples were collected at 1, 10, 30, 60, 120, and 240 minutes after administration. Samples were then centrifuged (14,000 rpm for 10 min) and mixed with an internal standard. Methanol was added and centrifuged (14,000 rpm for 10 min) to remove precipitates and evaporated to dryness with lyophilization. The dried samples were then reconstituted with methanol and injected into an Agilent 1100 LC/MSD with a Supelco Discovery HS C18 column (2.1×50 mm), and eluted with a linear gradient from 10% to 90% methanol in 0.1% aqueous trifluoroacetic acid at a flow rate of 0.2 mL/min and monitored by MS/MS. Drug concentrations in serum were calculated from peak area and extrapolated from prepared standards in serum with a lower limit of 10 nM. Area under the plasma concentration curve (AUC) was calculated by Prism 4.0 GraphPad, San Diego CA).

Pharmacodynamic (PD) study

C57BL/6 mice were intravenously injected with the unconjugated or PEGylated TLR7 ligands (200 nmol). Blood samples were collected 2, 4, 6, 24 48 or 72 hours after the injections. Sera were separated and kept at −20°C until use. The levels of IL-6 and TNF-α in the sera were measured by Luminex bead assay. The minimum detection levels of IL-6 and TNF-α were 5 pg/mL and 10 pg/mL, respectively.

Statistical Analysis

Prism 4.0 was used for statistical analyses including regression analyses. Data were plotted and fitted by nonlinear regression assuming a Gaussian distribution with uniform standard deviations between groups. The statistical differences were analyzed by two-way ANOVA with Bonferroni's *post hoc*, or Dunnett's *post hoc* testing. A value of $P < 0.05$ was considered statistically significant.

Results

Synthesis and characterization of PEGylated TLR7 ligand conjugates

Amide coupling of various sized amine/azide bifunctional PEGs with **1V209** in the presence of HATU and triethylamine yielded compounds **1a** and **2a** in greater than 90% yield. The formation of 1,2,3-triazoles were synthesized from compounds **1a** and **2a** through a copper catalyzed azide-alkyne Huisgen cycloaddition in the presence of 4-pentynoic acid to give compounds **1b** and **2b** in greater than 95% yield. Additionally, nitriles in compounds **1a** and **2a** were reduced to amines with Raney Ni and H_2 gas in MeOH to give compounds **1c** and **2c** in quantitative and 62% yield, respectively. Compound **3** was synthesized directly from **1V209** using HATU, triethylamine and *O,O′*-Bis(2-aminoethyl)octadecaethylene glycol in 29% yield. Coupling of various Sunbright® PEGs with **1V209**, HATU and triethylamine gave compounds **4**, **5**, **6** and **7** in greater than 80% yield.

Unconjugated compound **1V136** is highly insoluble in aqueous solution (Table 1). As PEG chains are hydrophilic, we postulated that its conjugation to **1V136** would improve the solubility, and possibly the bioavailability, of the compound (15). Hence, we tested the water solubility of selected PEGylated compounds (**1b** and **4**) and compared them to the unconjugated TLR7 ligands (**1V136**). Compound **1b** (240 mOsm/kg) was more soluble than **1V136** (less than 1mOsm/kg) (Table 1). Compound **4** was freely soluble in water, and a maximum solubility could not feasibly be determined. These data suggest that longer lengths of PEG chains provide better water solubility, as expected.

Many small molecules bind to serum carrier proteins, such as albumin and globulins, which influence tissue distribution and renal clearance (16,17). Hence, we performed experiments to measure the protein binding of selected PEGylated TLR7 ligands. Because the protein binding assay was only applicable to the compounds with molecular weights lower than 10,000 kDa due to the MW cutoff of the dialysis membrane, we studied compounds **1a**, **1b, 1c, 2a, 2b, 2c, 3,** and **4** (Table 1). Naproxen was used as a positive control. Percent protein binding of the compounds containing similar terminal groups, such as **1c**, **2c**, and **3**, were 51%, 58%, and 80 % respectively (Table 1). These data indicate that increasing the PEG chain length increases protein binding relative to **1V209** (Table 1).

In vitro NFkB activation and cytokine induction in murine cells

To test the agonistic activities of PEGylated TLR7 ligands *in vitro*, we used two murine cell types, NFκB-bla RAW 264.7 cells and primary BMDM (Table 2, Figure 1A, and 1B). The 50 percent of maximal effective concentration (EC50) and maximum level of induction (I_{max}) were assessed for each agent (Table 2). To compare the potencies of the conjugates, the I_{max}/EC50 ratios were calculated. In the experiments using the NFκB-bla RAW cell line, PEGylation progressively reduced potency compared to unconjugated ligand (**1V136**, Table 1). In contrast, when BMDM were analyzed in the same system, short chain PEG conjugates had reduced agonist activity, but the potency was restored when the PEG chains were 47 units or longer (compounds **4**, **5**, **6** and **7**, Table 2, Figure 1A and B, Supplementary Figure 1). Thus, the biological activities of the conjugates depended on the target cell, as well as the PEG length.

We also compared the terminal groups of the conjugates, which were amine, carboxylate, or azide. The PEGylated TLR7 ligand conjugates ending with amines or azides gave higher potency both in NFκB-bla RAW 264.7 cells and BMDM. In the preliminary experiments, neither unconjugated nor PEGylated TLR7 ligands induced detectable IL-6 or TNF-α in BMDM isolated from TLR7 deficient mice.

Cytokine induction by human PBMC

The previous experiments indicated that different cell types could have divergent responses to the TLR7 ligand conjugates. It was, therefore, of interest to study the activities of the PEGylated TLR7 ligands in human PBMC, as compared to mouse BMDM. The results showed that the PEGylated TLR7 ligands were 10-fold less potent cytokine stimulators in human PBMC, while the unconjugated **1V136** exerted similar activity in both species. Thus, the short PEGylated TLR7 ligands induced only minimal cytokines (IL-6 or TNF-α) in human PBMC at 1μM concentrations, which was an effective dose in murine cells. Only at 10μM concentrations was consistent cytokine production observed (Figure 2A–D). However, TLR7 ligand potency was restored in compound **4** containing 47 PEG units, for both human PBMC and murine BMDM. Compound **6,** which contains 271 PEG units, induced slightly less cytokines, but the difference was not significant. The conjugates with amine-terminals (**1c** and **2c**) exhibited higher potencies than the corresponding compounds with carboxyl-terminals (**1b** and **2b**).

Effects on human B cell proliferation by various PEGylated TLR7 ligands

TLR7 ligands directly activate human B cells and promote proliferation and expression of cytokine, and chemokine genes (18). To evaluate the capabilities of the PEGylated TLR7 ligands to induce human B cell proliferation, we incubated human PBMC from three independent donors with unconjugated or PEGylated TLR7 ligands for four days. The proliferation was determined by FACS analysis of CFSE dilution. The unconjugated TLR7 ligand (**1V136**) induced strong B cell proliferation at 1 μM (Figure 3A and 3F), consistent with its cytokine inducing effects at that concentration. Compounds **1b** and **2b** minimally induced proliferation at concentrations of 1 and 10 μM (Figure 3B, 3C, 3G, and 3H). Compounds **3** and **4** induced B cell proliferation only at 10 μM (Figure 3D, and 3E).

In vivo PK of various PEGylated TLR7 ligands

PEGylation with long chain influences the bioavailability and the circulation time of compounds *in vivo* (19). Hence, we examined the PK profiles of selected compounds with different PEG chain lengths. Mice were intravenously injected with 500 nmol **1V136**, **1b** (6-units) or **3** (18-units) and sera were collected at 1, 10, 30, 60, 120, and 240 min. The PK profiles of **1V136** and **1b** were similar (Figure 4A), whereas the longer PEG chain conjugate, **3**, showed higher area under the plasma concentration curve (AUC). Moreover, PEGylation increased the maximum serum concentration compared to the unconjugated compounds (Figure 4B). Thus, the 18-unit PEG conjugate (**3**) showed significantly higher maximum serum concentrations, compared to the unconjugated **1V136** molecule (Figure 4B).

In vivo cytokine induction by various PEGylated compounds

The experiments described above showed that PEGylation strongly influenced both the *in vitro* potency and the biochemical properties of the TLR7 ligands. Thus, it was important to determine if these changes influence the *in vivo* proinflammatory activities of the drugs. Mice were intravenously injected with 200 nmol **1b**, **1c**, **2b**, **3**, **4**, or **6** and sera was collected 2, 4, 6, 18, and 48 hours thereafter (Figure 5A and B). Conjugates with 6 and 10 PEG units (**1b**, **1c**, and **2b**) induced significantly less cytokine levels in serum at all time points analyzed, compared to the unconjugated **1V136** molecule. Conjugates with an amine terminal showed slightly higher TNF-α levels at 2 hours, compared to those with a carboxyl terminal. In contrast to the trend observed in the *in vitro* experiments, conjugates with longer PEG chains (i.e., 47 to 271) showed restored cytokine-inducing activity, to the levels of the unconjugated TLR7 ligands. Indeed, compound **6** (~271 PEG units) induced significantly higher levels of IL-6 and TNF-α at two hours after injection, compared to **1V136** itself (Figure 5B).

Discussion

PEGylation has been widely used to improve the pharmacokinetics of protein biologics, and ideally reduces the clearance and increases the half-life of the conjugated polypeptide (19,20). Conjugating PEG to low molecular weight drugs may also improve their solubility and extend their circulation time (15). We previously reported that adding 10-PEG unit chain to the insoluble TLR7 ligand, **1V136**, increases its solubility (19,20). However, PEGylation of the TLR7 ligand markedly reduced the agonistic activity of this molecule (11). TLR7 is located within the endosomal compartments of cells. Accordingly, cellular uptake and acidification of the endosome are important issues in determining the efficacy of TLR7 ligands. A goal of the current study was to assess the effects of PEG length on the solubility, pharmacokinetics and biologic activity of the TLR7 ligand. Our experiments revealed that conjugation of this TLR7 ligand to 6 or 10 PEG unit chains with a carboxyl terminus significantly reduced their proinflammatory activities both *in vitro* and *in vivo*. In

contrast, conjugation of the TLR7 ligand to longer PEG chains, containing ~47 to ~271 PEG units, restored and in some cases enhanced drug potency compared to the unconjugated TLR7 ligand.

Compound solubility can significantly influence the maximum serum concentration in a PK profile. In the studies of solubility and PK of the selected conjugates, we observed that longer PEG chains produced better solubility, as well as higher maximum plasma concentrations. Compound **3**, with18 PEG units, showed the highest AUC among the tested agents (Figure 4). These data are consistent with other studies, which have shown that PEG chains with higher molecular weights gradually yield greater bioavailability and a longer circulating half-life compared to those of lower molecular weight (21). PEGylated compounds may exhibit a prolonged *in vivo* circulation time because of reduced liver and renal clearance (22,23).

Although PEGylation can stabilize a drug and prolong it's *in vivo* half-life, it can also decrease biological activity by shielding a drug from its intended target. Thus, a decrease in potency is often observed for PEGylated peptides and low molecular weight proteins (24,25). In our study, the cytokine inducing activity of the TLR7 ligands was significantly decreased by conjugation with low molecular weight PEG chains, but was restored by conjugation to longer PEG chains, at least in primary bone marrow derived macrophages and human blood mononuclear cells. The decreased activity by short chain PEGylation could be ascribed to factors such as 1) inhibition of the cellular uptake of the agonist, and its transport to endosomal TLR7, 2) steric hindrance of binding to the receptors, and 3) effects of PEG chains on endosomal stability. However, because the PEGylated conjugates with longer PEG chains had potent activities, the latter two mechanisms seem unlikely. The fact that conjugates with 18 or longer PEG units showed equivalent activities to the unconjugated **1V136**, indicates that the chemical modification of the drug by PEGylation did not block its interaction with the TLR7 target molecule.

The biphasic effect of PEGylation observed in primary macrophages mimicked the *in vivo* activities of the compounds. As expected from the relative potencies obtained from *in vitro* studies, the TLR7 ligands conjugated to 6 or 10 PEG unit chains (**1a**, **1b**, **1c**, **2a**, **2b**, and **2c**) exhibited minimum induction of proinflammatory cytokines in mice (Figure 5), despite the drug's improved circulation time. Although we believe that endosomal delivery mainly explains these results, there could be additional mechanisms unique to the *in vivo* setting, including altered distribution of the various conjugates among the components in the reticuloendothelial system, such as liver and spleen, where many TLR7 expressing cells reside.

The activity profiles of the conjugates towards human peripheral blood mononuclear cells were similar to those observed in murine macrophages (Figure 2). Similar trends were observed in the effects of the conjugates on B cell proliferation, a known effect of TLR7 activation *in vivo*. Notably, human B cell proliferation by compounds **1b** and **2b** was undetectable in the three independent donors.

In summary, these experiments indicate that PEG conjugation can significantly influence both the *in vitro* and *in vivo* activities of the TLR7 ligands. The long chain conjugates have both agonist activity and high solubility, while the short chain conjugates are nearly inactive. TLR7 is uniquely located in the endosomal intracellular compartment. Activation of TLR7 signaling requires uptake and proteolytic processing in the endosomes. Furthermore, recent reports indicate that TLR7 is present not only in immune cells, but also in non-immune cells, such as corneal and colonic epithelium (26,27). The unique properties of this receptor make it difficult to predict the outcome of formulation and conjugation of TLR7 ligands. We

propose here that PEGylation to TLR7 ligand can provide benefits in two distinct ways; 1) conjugation to short 6 to 10 PEG unit chains may create partial agonists with low potency that may be useful for antagonistic applications, and 2) conjugation to longer PEG chains can increase their agonistic potency, and may be useful for adjuvant applications. PEG chains are essentially nontoxic. Many PEG conjugates, and the TLR7 agonist Imiquimod, are FDA approved. Improvement of the pharmaceutical properties of TLR7 ligands using PEGylation could be a feasible methodology to enhance drug delivery, and alter immunologic properties for human use.

Supplementary Material

Refer to Web version on PubMed Central for supplementary material.

Acknowledgments

Abbreviations

TLR	Toll like receptor
IL	interleukin
TNF	tumor necrosis factor
LPS	lipopolysaccharide
MyD88	myeloid differentiation primary response gene 88
PBMC	peripheral blood mononuclear cells
PEG	polyethylene glycol
EtOH	ethanol
THF	tetrahydrofuran
DOPE	1,2-Dioleoyl-sn-glycero-3-phosphoethanolamine
DMF	N,N-Dimethylformamide
HATU	O-(7-Azabenzotriazol-1-yl)-N,N,N′,N′-tetramethyluroniumhexafluorophosphate
DCM	dichloromethane
TEA	triethylamine
pDC	plasmacytoid dendritic cells
OVA	ovalbumin
CFSE	carboxy-fluoresceindiacetate succinimidyl ester

References

1. Akira S, Hemmi H. Recognition of pathogen-associated molecular patterns by TLR family. Immunol Lett. 2003; 85:85–95. [PubMed: 12527213]

2. Akira S. TLR signaling. Curr Top Microbiol Immunol. 2006; 311:1–16. [PubMed: 17048703]

3. Akira S, Takeda K. Toll-like receptor signalling. Nat Rev Immunol. 2004; 4:499–511. [PubMed: 15229469]

4. Diebold SS, Kaisho T, Hemmi H, Akira S, Reis e Sousa C. Innate antiviral responses by means of TLR7-mediated recognition of single-stranded RNA. Science. 2004; 303:1529–31. [PubMed: 14976261]

5. Lee J, Chuang TH, Redecke V, She L, Pitha PM, Carson DA, Raz E, Cottam HB. Molecular basis for the immunostimulatory activity of guanine nucleoside analogs: activation of Toll-like receptor 7. Proc Natl Acad Sci U S A. 2003; 100:6646–51. [PubMed: 12738885]

6. Lee J, Mo JH, Katakura K, Alkalay I, Rucker AN, Liu YT, Lee HK, Shen C, Cojocaru G, Shenouda S, Kagnoff M, Eckmann L, Ben-Neriah Y, Raz E. Maintenance of colonic homeostasis by distinctive apical TLR9 signalling in intestinal epithelial cells. Nat Cell Bio. 2006; 8:1327–36. [PubMed: 17128265]

7. Hemmi H, Kaisho T, Takeuchi O, Sato S, Sanjo H, Hoshino K, Horiuchi T, Tomizawa H, Takeda K, Akira S. Small anti-viral compounds activate immune cells via the TLR7 MyD88-dependent signaling pathway. Nat Immunol. 2002; 3:196–200. [PubMed: 11812998]

8. Kurimoto A, Ogino T, Ichii S, Isobe Y, Tobe M, Ogita H, Takaku H, Sajiki H, Hirota K, Kawakami H. Synthesis and evaluation of 2-substituted 8- hydroxyadenines as potent interferon inducers with improved oral bioavailabilities. Bioorg Med Chem. 2004; 12:1091–9. [PubMed: 14980621]

9. Sepulveda FE, Maschalidi S, Colisson R, Heslop L, Ghirelli C, Sakka E, Lennon-Dumenil AM, Amigorena S, Cabanie L, Manoury B. Critical role for asparagine endopeptidase in endocytic Toll-like receptor signaling in dendritic cells. Immunity. 2009; 31:737–48. [PubMed: 19879164]

10. Wu CC, Hayashi T, Takabayashi K, Sabet M, Smee DF, Guiney DD, Cottam HB, Carson DA. Immunotherapeutic activity of a conjugate of a Toll-like receptor 7 ligand. Proc Natl Acad Sci U S A. 2007; 104:3990–5. [PubMed: 17360465]

11. Chan M, Hayashi T, Kuy CS, Gray CS, Wu CC, Corr M, Wrasidlo W, Cottam HB, Carson DA. Synthesis and immunological characterization of toll-like receptor 7 agonistic conjugates. Bioconjug Chem. 2009; 20:1194–200. [PubMed: 19445505]

12. Parikh HH, Balasubramanian VV, Chu WL, Morris ME, Ramanathan M. Rapid Solubility Determination Using Vapor-Phase Osmometry. J Biomol Screen. 1999; 4:315–318. [PubMed: 10838428]

13. Hayashi T, Rao SP, Takabayashi K, Van Uden JH, Kornbluth RS, Baird SM, Taylor MW, Carson DA, Catanzaro A, Raz E. Enhancement of innate immunity against Mycobacterium avium infection by immunostimulatory DNA is mediated by indoleamine 2,3-dioxygenase. Infect Immun. 2001; 69:6156–64. [PubMed: 11553555]

14. Datta SK, Redecke V, Prilliman KR, Takabayashi K, Corr M, Tallant T, DiDonato J, Dziarski R, Akira S, Schoenberger SP, Raz E. A Subset of Toll-Like Receptor Ligands Induces Cross-presentation by Bone Marrow-Derived Dendritic Cells. Journal of Immunology. 2003; 170:4102–4110.

15. Pepinsky RB, Lee WC, Cornebise M, Gill A, Wortham K, Chen LL, Leone DR, Giza K, Dolinski BM, Perper S, Nickerson-Nutter C, Lepage D, Chakraborty A, Whalley ET, Petter RC, Adams SP, Lobb RR, Scott DM. Design, synthesis, and analysis of a polyethelene glycol-modified (PEGylated) small molecule inhibitor of integrinα4β1 with improved pharmaceutical properties. J Pharmacol Exp Ther. 2005; 312:742–50. [PubMed: 15485895]

16. Dill KA, Shortle D. Denatured states of proteins. Annu Rev Biochem. 1991; 60:795–825. [PubMed: 1883209]

17. Dockal M, Carter DC, Ruker F. Conformational transitions of the three recombinant domains of human serum albumin depending on pH. J Biol Chem. 2000; 275:3042–50. [PubMed: 10652284]

18. Hanten JA, Vasilakos JP, Riter CL, Neys L, Lipson KE, Alkan SS, Birmachu W. Comparison of human B cell activation by TLR7 and TLR9 agonists. BMC Immunol. 2008; 9:39. [PubMed: 18652679]

19. Greenwald RB. PEG drugs: an overview. J Control Release. 2001; 74:159–71. [PubMed: 11489492]

20. Greenwald RB, Choe YH, McGuire J, Conover CD. Effective drug delivery by PEGylated drug conjugates. Adv Drug Deliv Rev. 2003; 55:217–50. [PubMed: 12564978]

21. Kaminskas LM, Boyd BJ, Karellas P, Krippner GY, Lessene R, Kelly B, Porter CJ. The impact of molecular weight and PEG chain length on the systemic pharmacokinetics of PEGylated poly l-lysine dendrimers. Mol Pharm. 2008; 5:449–63. [PubMed: 18393438]

22. Kaminskas LM, Kelly BD, McLeod VM, Boyd BJ, Krippner GY, Williams ED, Porter CJ. Pharmacokinetics and tumor disposition of PEGylated, methotrexate conjugated poly-l-lysine dendrimers. Mol Pharm. 2009; 6:1190–204. [PubMed: 19453158]

23. Kaminskas LM, Kota J, McLeod VM, Kelly BD, Karellas P, Porter CJ. PEGylation of polylysine dendrimers improves absorption and lymphatic targeting following SC administration in rats. J Control Release. 2009; 140:108–16. [PubMed: 19686787]

24. Esposito P, Barbero L, Caccia P, Caliceti P, D'Antonio M, Piquet G, Veronese FM. PEGylation of growth hormone-releasing hormone (GRF) analogues. Adv Drug Deliv Rev. 2003; 55:1279–91. [PubMed: 14499707]

25. Bowen S, Tare N, Inoue T, Yamasaki M, Okabe M, Horii I, Eliason JF. Relationship between molecular mass and duration of activity of polyethylene glycol conjugated granulocyte colony-stimulating factor mutein. Exp Hematol. 1999; 27:425–32. [PubMed: 10089904]

26. Dhanasekaran S, Kannan TA, Dhinakar Raj G, Tirumurugaan KG, Raja A, Kumanan K. Differential expression of toll-like receptor mRNA in corneal epithelium of ruminants. Vet Ophthalmol. 2010; 13:270–4. [PubMed: 20618807]

27. Grimm M, Kim M, Rosenwald A, Heemann U, Germer CT, Waaga-Gasser AM, Gasser M. Toll-like receptor (TLR) 7 and TLR8 expression on CD133+ cells in colorectal cancer points to a specific role for inflammation-induced TLRs in tumourigenesis and tumour progression. Eur J Cancer. 2010; 46:2849–57.
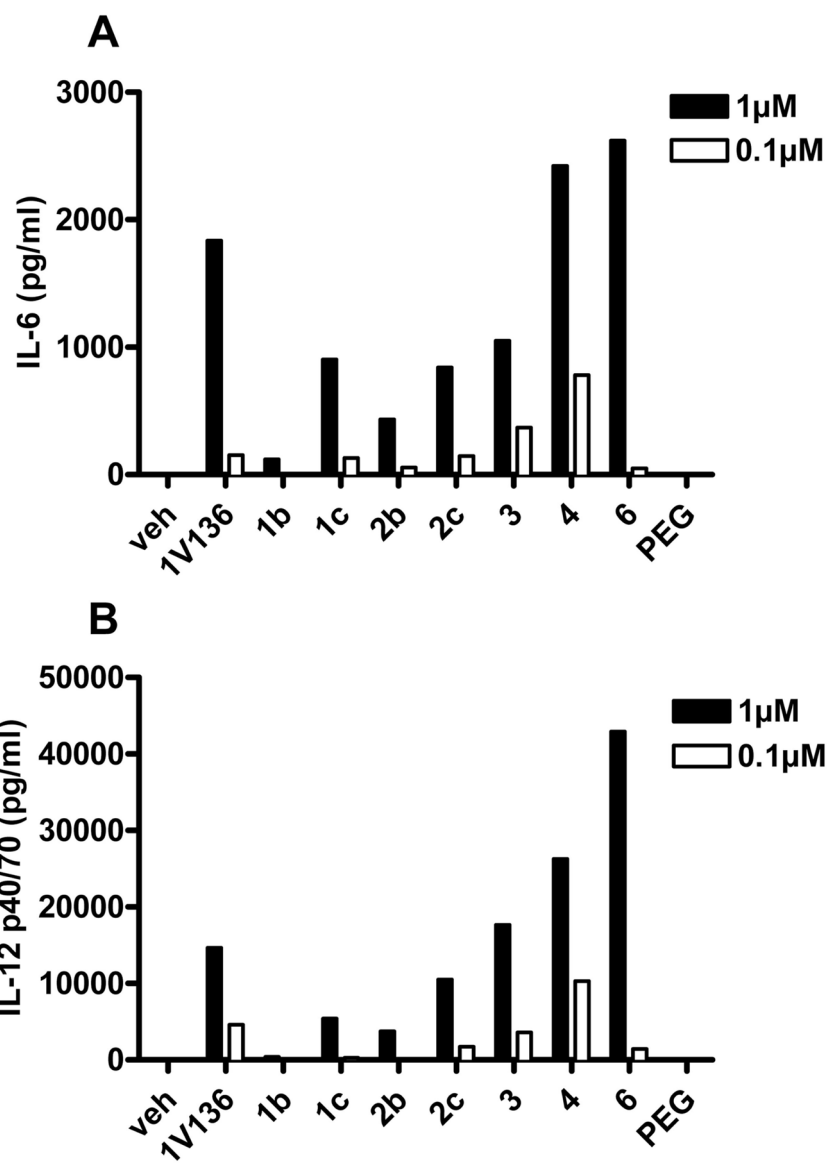
Figure 1.
In vitro pro-inflammatory profiles in murine BMDM. Murine primary BMDM were incubated with serially diluted PEGylated TLR7 ligands. The levels of IL-6 and IL-12 released in the culture supernatants were determined by ELISA. Data were plotted and fitted by nonlinear regression using Prism software (Supplementary Figure 1). The data are representative of two independent experiments. The levels of IL-6 (A) and IL-12 (B) by 1 μM and 0.1 μM were interpolated using Prism software.
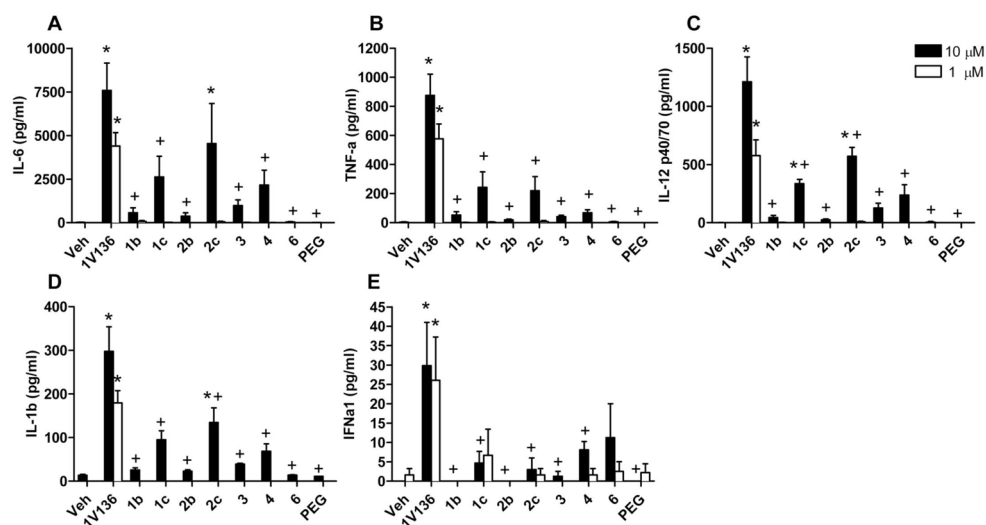
Figure 2.
Cytokine/chemokines inducing activities in human PBMC. Human PBMC were incubated with 10 μM (black bar) or 1 μM (open bar) PEGylated TLR7 ligands for 18 hours. The levels of cytokines and chemokines were evaluated by Luminex immunoassays. Data shown are means ± SEM of data from three individuals. * and + denote $p < 0.05$ compared to vehicle and 1V136 respectively using one-way ANOVA with Dunnett's post hoc testing.
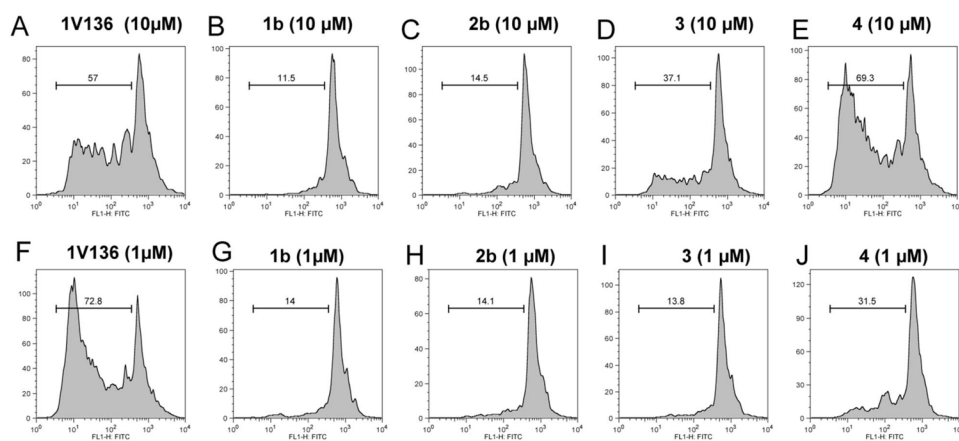
Figure 3.
Effects on human B lymphocyte proliferation. CFSE labeled human PBMC were prepared as described in the Methods, and were incubated with 10 µM (A, B, C, D and E) or 1 µM (F, G, H, I, and J) compounds for 18 hours. B cells were identified by surface CD19 expression. Cell proliferation of the CD19 gated B cell population was evaluated by FACS assay and is shown as a histogram. The data are representative of two independent experiments.
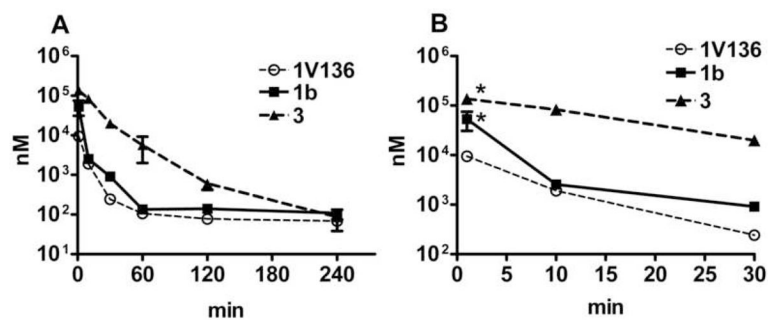
Figure 4.
In vivo PK study of various PEGylated compounds. C57BL/6 mice (n=3) were injected i.v. with 500 nmol PEGylated TLR7 ligands, and blood samples were collected at 1, 10, 30, 60, 120, and 240 min after administration. Drug concentrations (nM) were determined using an internal standard. The data shown are pooled from three independent experiments. The data plotted shows 0 to 240 min (A) and 0 to 30 min (B). AUC of 1V136, 1b and 3 are 97246 ± 10431, 355900 ± 231915, and 2483531 ± 222049, respectively. Data shown are pooled from two independent experiment. * denotes $p < 0.05$ compared to 1V136 by one-way ANOVA with Dunnett's post hoc testing.
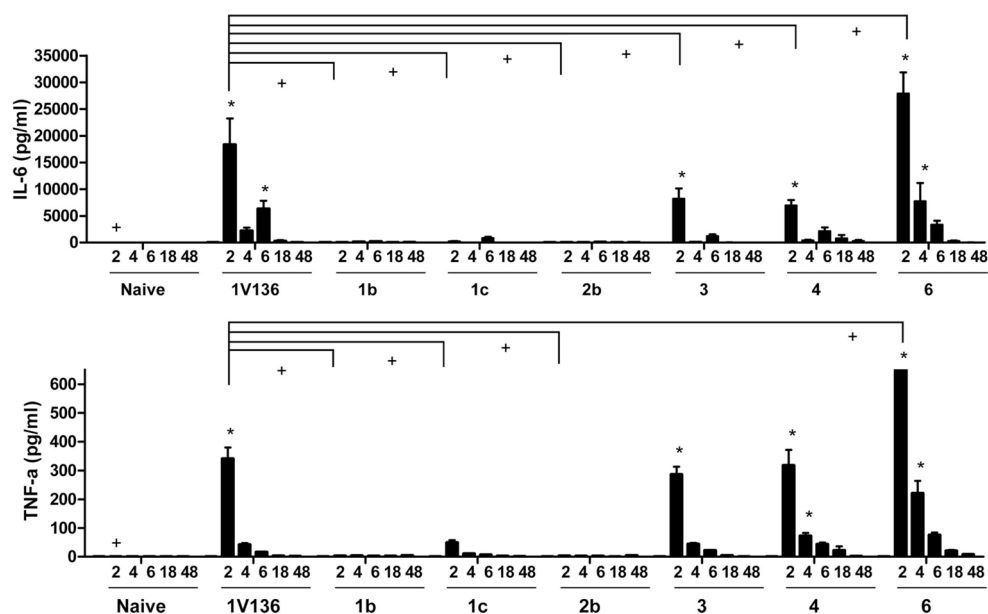
Figure 5.
In vivo PD study of various PEGylated TLR7 ligand conjugates. The in vivo kinetics of proinflammatory cytokine induction by PEGylated TLR7 ligands were determined after intravenous injection of C57BL/6 mice (n = 5 per group) with 200 nmol unconjugated or PEGylated TLR7 ligand conjugates. Serum samples were collected 2, 4, 6, 24, and 48 hours after injection. The levels of TNFa (A) and IL-6 (B) were measured by Luminex assay. Data are means ± SEM of five mice and are representative of two independent experiments. * and + denote p< 0.05 compared to the vehicle-treated and 1V136-treated mice, respectively, by one-way ANOVA tests with Bonferroni post hoc testing.
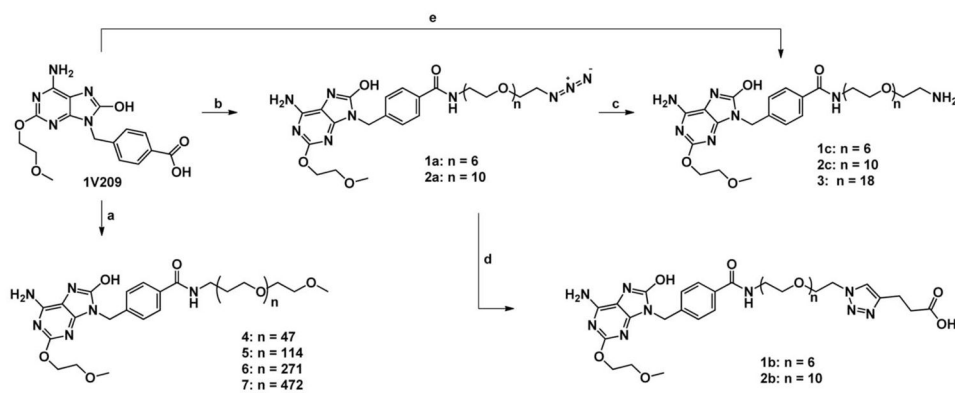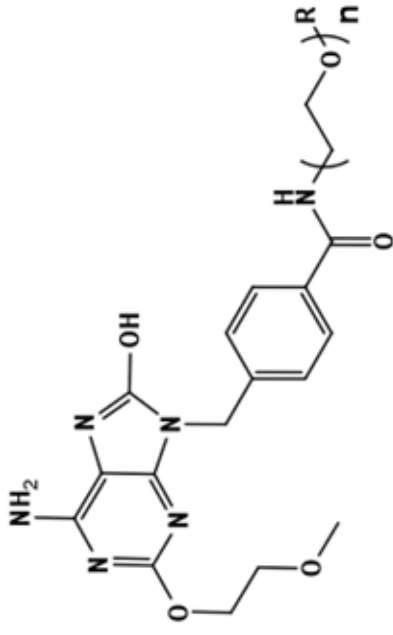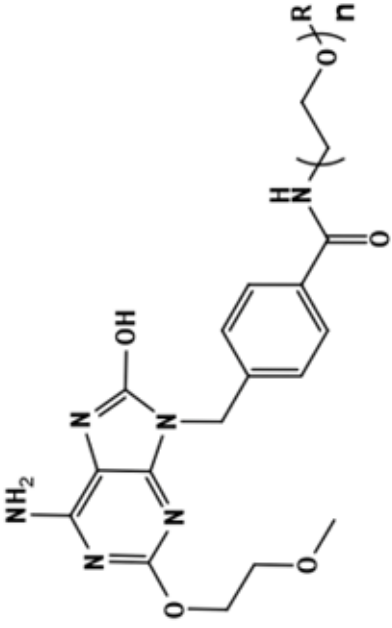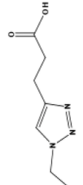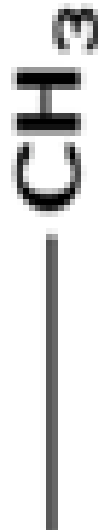
Scheme 1.
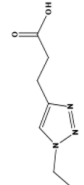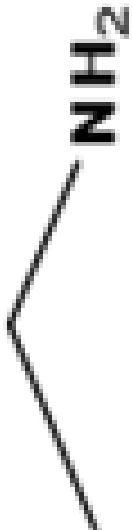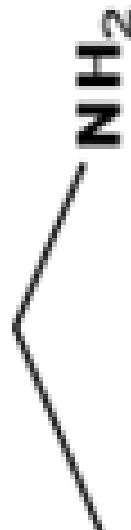Conjugation of TLR7 ligand to PEG chain. (a) Appropriate PEG (Sunbright® MEPA-20H, Sunbright® MEPA-50H, Sunbright® MEPA-12T, Sunbright® MEPA-20T), HATU, triethylamine, DMF, DCM, r.t.; (b) Appropriate PEG (O-(2-Aminoethyl)-O′-(2-azidoethyl)pentaethylene glycol, O-(2-Aminoethyl)-O′-(2-azidoethyl)nonaethylene glycol), HATU, triethylamine, DMF, r.t.; (c) Raney Ni, H2, MeOH, r.t.; (d) 4-pentynoic acid, sodium ascorbate, Cu(OAc)2, t-BuOH/H2O/THF 2:2:1, r.t; (e) O,O′-Bis(2-aminoethyl)octadecaethylene glycol, HATU, triethylamine, DMF, r.t.
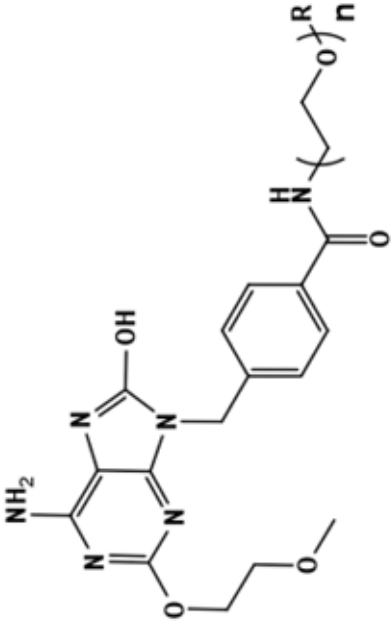
Table 1

Structure of PEGylated TLR7 ligands

Compound Name	R	MW	Protein Binding (%)	Water Solubility (mOsm/kg)
1V136	H	691.33	66.8 ± 1.3	<1
1V209	COOH	789.83	25.4 ± 1	35 ±1

Compound Name	n	R	MW	% Protein Binding	Water Solubility
1a	6		691.33	37.1 ± 1.5	nd^c

Compound Name	n	R	MW	% Protein Binding	Water Solubility
1b	6		789.83	49.6 ± 1.9	240 ± 10
1c	6		665.74	51.3 ±6.4	nd[c]
2a	10		867.43	44.5 ±0.5	nd[c]
2b	10		966.04	48.2 ±5.9	>1000
2c	10		841.95	57.6 ± 1.2	nd[c]
3	18		1238.42	79.5 ± 1.35	nd[c]
4	47[a]		2525.13[a]	89.7 ± 1	>1000

Compound Name	n	R	MW	% Protein Binding	Water Solubility
5	114^a	CH_3	5572.13^a	nd^b	nd^c
6	271^a	CH_3	12609.13^a	nd^b	nd^c
7	472^a	CH_3	21701.13^a	nd^b	nd^c

[a] Approximate molecular weight due to heterogeneity of PEG polymer

[b] Compounds 5, 6 and 7 exceeded the maximum molecular weight for the equilibrium dialysis membrane,

[c] Solubility was determined for readily available compounds.

Table 2

In vitro proinflammatory profiles in NF B-bla RAW cells and murine primary BMDM

	PEG Chain length	Terminal group	EC50[a]		Imax		Imax/EC50	
			NFkB–RAW[b] (µM)	BMDM[c] (µM)	NFkB–RAW (RR)	BMDM (IL-6 ng/ml)	NFkB–RAW	BMDM
1V136	0		0.08 ± 0.01	0.36 ± 0.09	3.56 ± 0.38	3.32 ± 0.54	46.79 ± 5.02	8.86 ± 0.71
1a	6	N3	$4.13 \pm 0.97*$	$8.18 \pm 1.91*$	2.90 ± 0.06	2.60 ± 0.49	$0.70 \pm 0.01*$	$0.35 \pm 0.07*$
1b	6	COOH	$4.99 \pm 0.70*^{c})$	$10.58 \pm 1.74*$	3.04 ± 0.23	2.46 ± 0.36	$0.61 \pm 0.05*$	$0.23 \pm 0.04*$
1c	6	NH2	1.19 ± 0.20	3.90 ± 1.06	3.27 ± 0.39	5.19 ± 1.96	$2.74 \pm 0.32*$	$1.33 \pm 0.50*$
2a	10	N3	$5.91 \pm 1.33*$	$6.93 \pm 3.54*$	3.55 ± 0.14	2.72 ± 0.34	$0.60 \pm 0.02*$	0.39 ± 0.05
2b	10	COOH	2.67 ± 0.75	$4.42 \pm 1.18*$	3.15 ± 0.23	2.79 ± 0.47	$1.18 \pm 0.09*$	$0.64 \pm 0.15*$
PEG 2c	10	NH2	1.16 ± 0.39	2.24 ± 0.33	3.23 ± 0.27	2.89 ± 0.49	$2.78 \pm 0.23*$	$1.21 \pm 0.14*$
3	18	NH2	0.90 ± 0.29	1.79 ± 0.77	3.58 ± 0.58	4.10 ± 1.33	$3.98 \pm 0.64*$	2.71 ± 0.86
4	47	OMe	1.12 ± 0.31	0.37 ± 0.23	4.17 ± 0.51	2.11 ± 0.08	$3.74 \pm 0.46*$	5.68 ± 0.22
5	114	OMe	2.20 ± 0.09	0.11 ± 0.01	4.86 ± 0.08	3.93 ± 0.65	$2.21 \pm 0.36*$	$34.75 \pm 5.71*$
6	271	OMe	$10.84 \pm 4.08*$	0.38 ± 0.09	N/A	3.93 ± 0.61	N/A	10.31 ± 1.59
7	472	OMe	$12.67 \pm 2.39*$	0.81 ± 0.21	N/A	3.20 ± 0.39	N/A	3.97 ± 0.48

[a]EC50 was calculated using Prism software.

[b]NFκB Activation was measured using NFkB-bla RAW cells. The results were expressed as response ratio (RR).

[c]*denotes p<0.05 compared to 1V136 using one-way ANOVA with Dunnett's post hoc testing.